

CHIMERAS IN PHASE OSCILLATOR NETWORKS LOCALLY COUPLED THROUGH AN AUXILIARY FIELD: STABILITY AND BIFURCATIONS

CARLO R. LAING

ABSTRACT. We study networks in the form of a lattice of nodes with a large number of phase oscillators and an auxiliary variable at each node. The only interactions between nodes are nearest-neighbour. The Ott/Antonsen ansatz is used to derive equations for the order parameters of the phase oscillators at each node, resulting in a set of coupled ordinary differential equations. Chimeras are steady states of these equations and we follow them as parameters are varied, determining their stability and bifurcations. In two-dimensional domains, we find that spiral wave chimeras and rotating waves have significantly different properties than those in networks with nonlocal coupling.

Chimeras are unusual spatiotemporal patterns in networks of oscillators characterised by having some oscillators synchronised while the remainder are incoherent. Many studies of chimeras involve networks with nonlocal coupling, while a few consider only local coupling. Most of the studies of locally coupled networks show just the results of numerical simulations. We consider networks of phase oscillators with local interactions through an auxiliary field. Using the Ott/Antonsen ansatz we derive and study equations for the dynamics of such networks, determining the stability and bifurcations of chimera states. In several cases we find fundamental differences between solutions in locally coupled and nonlocally coupled networks.

1. INTRODUCTION

Chimeras are spatiotemporal patterns in networks of oscillators for which some oscillators synchronise while the others are incoherent, even though the oscillators are identical or statistically identical [1, 2]. Such patterns have less symmetry than the network which supports them. Chimeras have been studied intensively for more than a decade and observed in a number of physical systems [3, 4]. One of the most significant advances in the study of chimeras was the use of the Ott/Antonsen ansatz [5, 6] which gave an exact dimension reduction for infinite networks of sinusoidally coupled phase oscillators, such as the Kuramoto model [7, 8]. For example, this ansatz allows one to describe the eventual dynamics of two coupled (infinite) networks by a pair of complex-valued ordinary differential equations [9, 10].

Chimeras were first reported in systems with nonlocal coupling [11, 12, 13] and for some time it was thought that such coupling was necessary in order that such states could be observed [14]. However, in 2015 Laing [15] showed numerically that chimeras could exist in systems with purely local coupling, considering three systems which could be thought of as approaching nonlocally coupled systems in a particular limit.

Since this first report of chimeras in systems with purely local coupling [15], many other authors have reported chimeras in systems with only local coupling [16, 17, 18,

Date: May 2, 2023.

Key words and phrases. chimera, coupled oscillators, reaction-diffusion.

19]. Some have studied systems where each node in isolation has complex dynamics (e.g. bursting [20]) or is bistable [21, 22, 23]. Others have considered reaction-diffusion type systems [24, 25, 26] similar to those whose analysis gave rise to early observations of chimeras [11, 13]. However, all of these previous papers have shown just the results of numerically integrating the equations describing a dynamical system, for a finite amount of time. While the accuracy of numerical integration can be controlled, there is the possibility that some of the observed chimeras may actually be long-lived transients [27]. Any exploration of parameter space has resulted in a fairly coarse partitioning of that space based on the stable patterns observed (often with no or limited exploration of dependence on initial conditions), and no analysis of the bifurcations creating or destroying chimeras has been undertaken.

To overcome these issues, here we revisit several of the models in [15] and show that they can be analysed using the Ott/Antonsen ansatz, which can be used to determine the stability of the chimeras found there, not just their existence. Such solutions can be followed as parameters are varied, and bifurcations of them characterised. We also consider a two-dimensional network with only local coupling which supports spiral wave chimeras, and an annular domain which supports rotating waves, which have similarities to spiral wave chimeras.

All of the models studied here have a common form: the network is formed from a lattice of nodes, and at each node there is a large number of phase oscillators and a single auxiliary variable, which may be real or complex. The phase oscillators at a node are influenced by the value of the auxiliary variable, which in turn is driven by some form of average over the states of the phase oscillators. The only interactions between nodes is nearest-neighbour, involving only the auxiliary variables. A number of other authors have considered networks of oscillators interacting diffusively through a medium [28, 29, 30, 31] and we discuss some of them further below.

The structure of the paper is as follows. Sec. 2 considers a one-dimensional network of Kuramoto phase oscillators, as studied in [15]. In Sec. 2.1 we consider asymmetric local coupling in this model, which results in the chimera moving at a constant speed. In Sec. 3 we consider Winfree oscillators on a one-dimensional domain, as studied in [15]. In Secs. 4 and 5 we consider Kuramoto oscillators on two-dimensional domains in the shapes of a square and an annulus, respectively.

2. KURAMOTO OSCILLATORS IN 1D

The first model we consider consists of N communities of oscillators equally-spaced on a domain of length L with periodic boundary conditions, similar to that in [32]. Each community consists of M phase oscillators and also has a complex variable z associated with it. The governing equations are

$$(1) \quad \frac{d\theta_j^k}{dt} = \omega_j^k - \text{Re} \left(z_j e^{-i\theta_j^k} \right)$$

$$(2) \quad \epsilon \frac{dz_j}{dt} = \frac{Ae^{i\beta}}{M} \sum_{k=1}^M e^{i\theta_j^k} - z_j + \frac{z_{j+1} - 2z_j + z_{j-1}}{(\Delta x)^2}$$

for $j = 1, 2, \dots, N$ and $k = 1, 2, \dots, M$, where θ_j^k is the phase of the k th oscillator in community j , $\Delta x = L/N$, and A, β and ϵ are all constants. For each j and k , ω_j^k is randomly chosen from a Lorentzian distribution with half-width-at-half-maximum σ

centred at ω_0 , namely

$$(3) \quad g(\omega) = \frac{\sigma/\pi}{(\omega - \omega_0)^2 + \sigma^2}$$

Thus each phase oscillator in population j is influenced by the value of z_j , and z_j is driven by the mean over k of the $e^{i\theta_j^k}$, the classical Kuramoto order parameter. Note that the only coupling is nearest-neighbour between communities, through the variable z . The last term in (2) is clearly a finite-difference approximation to $\partial^2 z / \partial x^2$.

An example of a chimera solution of (1)-(2) is shown in Fig. 1. For simplicity the phase of only one phase oscillator in each community is shown. The phases θ_j^1 have clearly separated into a largely synchronous group and an asynchronous group, characteristic of a chimera, while the z_j vary relatively smoothly in space over the whole domain. The time-averaged frequencies of the oscillators also vary smoothly in space, as required for a chimera (not shown).

Letting $M \rightarrow \infty$ we can use the Ott/Antonsen ansatz [5, 6] to describe the dynamics of the phase oscillator density in each community. Defining

$$(4) \quad a_j = \lim_{M \rightarrow \infty} \frac{1}{M} \sum_{k=1}^M e^{i\theta_j^k}$$

then using standard calculations [1] we have

$$(5) \quad \frac{da_j}{dt} = -(\sigma - i\omega_0)a_j - (i/2)(z_j + \bar{z}_j a_j^2)$$

and (2) becomes

$$(6) \quad \epsilon \frac{dz_j}{dt} = Ae^{i\beta} a_j - z_j + \frac{z_{j+1} - 2z_j + z_{j-1}}{(\Delta x)^2}$$

As explained in [15], the motivation for studying (1)-(2) comes from considering the case $\epsilon = 0$. If a_j is the j th entry of the vector \mathbf{a} and similarly for z_j , setting $\epsilon = 0$ in (6) allows us to solve for \mathbf{z} in terms of \mathbf{a} :

$$(7) \quad \mathbf{z} = Ae^{i\beta}(I - D)^{-1}\mathbf{a}$$

where I is the $N \times N$ identity matrix and D is the classical second difference operator on N points with periodic boundary conditions. The matrix $(I - D)^{-1}$ can be found explicitly and has no non-zero entries, and inserting (7) into (5) we obtain an equation for the a_j with nonlocal coupling.

Eqns. (1)-(2) are invariant under a shift of all θ_j^k by a constant and rotation of all z_j in the complex plane by the same amount, and thus we go to a uniformly rotating coordinate frame in which the solutions of (5)-(6) of interest (chimeras) are stationary. Letting $b_j = a_j e^{-i\Omega t}$ and $y_j = z_j e^{-i\Omega t}$, where Ω is the (unknown) speed of rotation, we obtain

$$(8) \quad \frac{db_j}{dt} = -(\sigma - i(\omega_0 - \Omega))b_j - (i/2)(y_j + \bar{y}_j b_j^2)$$

$$(9) \quad \epsilon \frac{dy_j}{dt} = Ae^{i\beta} b_j - y_j + \frac{y_{j+1} - 2y_j + y_{j-1}}{(\Delta x)^2} - i\epsilon \Omega y_j$$

We are interested in steady states of these equations. An example is shown in Fig. 2 for the same parameters as used in Fig. 1. b_j and y_j are smooth functions of the spatial index j . Recall the interpretation of $|b_j|$: it is equal to $|a_j|$ (4), and $|b_j| = 1$ corresponds to synchronous oscillators (the distribution of phases is a Dirac delta function) while $|b_j| = 0$

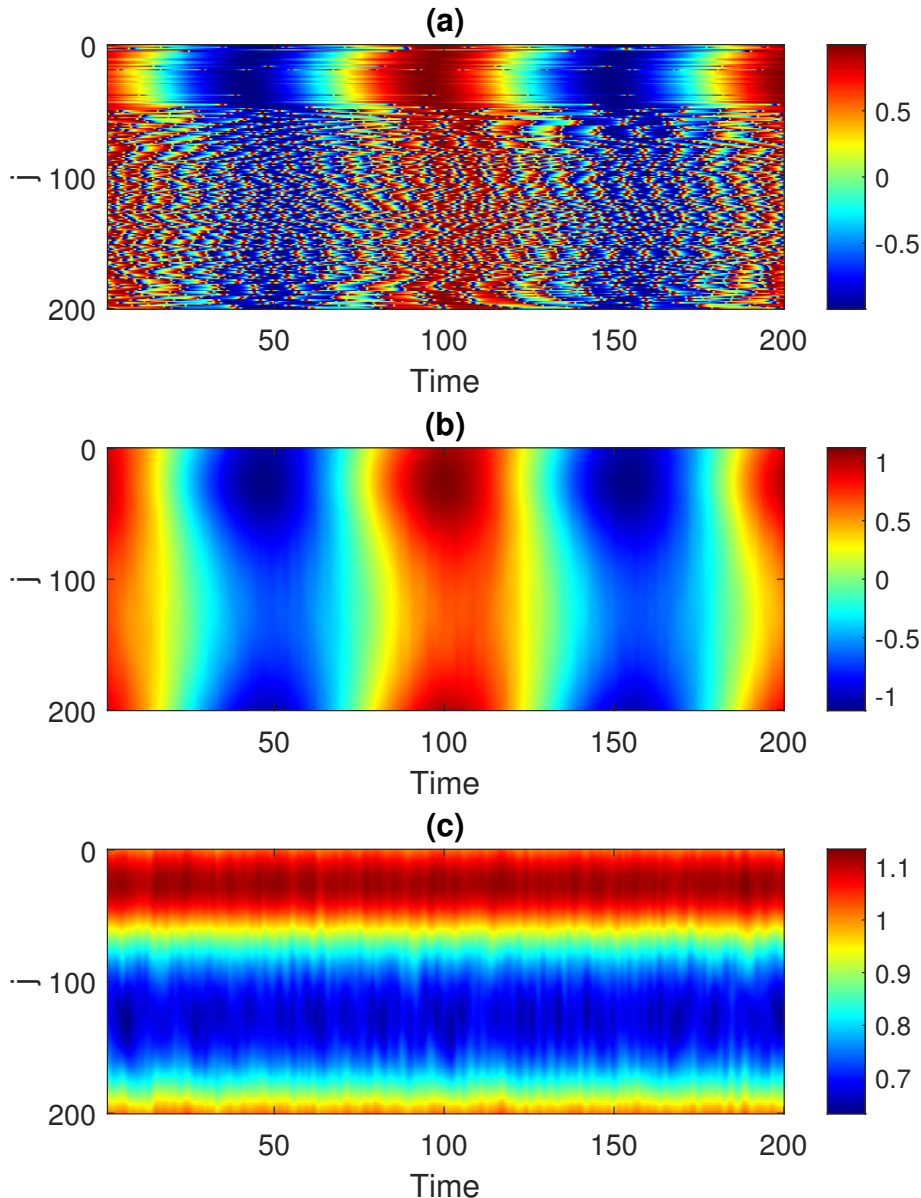


FIGURE 1. Chimera solution of the system (1)-(2). (a): $\sin \theta_j^1$; (b): $\sin(\arg(z_j))$; (c): $|z_j|$. Parameters: $\omega_0 = 1, \sigma = 0.01, \epsilon = 0.2, A = 1.5, L = 2\pi, N = 200, M = 20, \beta = 0.1$.

corresponds to a uniform angular distribution of phases, i.e. complete asynchrony. Due to the frequency heterogeneity in the network, i.e. the nonzero value of σ , $|b_j|$ never reaches 1, but the plateau centred at $j = 100$ in Fig. 2 corresponds to the largely synchronous group seen for values of j centred at $j \approx 30$ in Fig. 1(a).

We could find the steady state of (8)-(9) by setting the right hand side of (8) to zero and solving the resulting quadratic in b_j (choosing the solution for which $|b_j| \leq 1$), then setting the right hand side of (9) to zero and inserting the value of b_j just found. This gives an equation equivalent to equation (15) in [15]. However, that is an equation just characterising a steady state, if it exists, and gives no information about the stability of this solution. In contrast, here we linearise (8)-(9) about such a steady state in order to determine its stability.

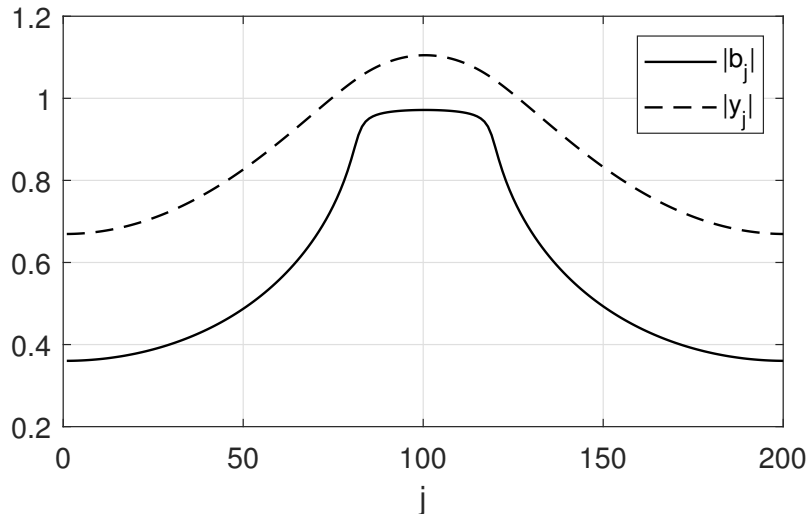


FIGURE 2. Steady state of (8)-(9) with $\Omega = -0.049437$. Parameters as in Fig. 1.

We explore the effects of varying both ϵ and β . Increasing either ϵ or β from the values used in Fig. 1 we find the stable chimera is destroyed in a saddle-node bifurcation. Following this bifurcation as both ϵ and β are varied we obtain the blue solid curve in Fig. 3. The stable chimera also undergoes a Hopf bifurcation which, from numerical simulations of (8)-(9), seems to be subcritical. The curve of Hopf bifurcations is shown dashed red in Fig. 3. Moving away from the nonlocally coupled case (i.e. increasing ϵ) the range of β values for which a chimera exists decreases.

In recent work [29], Bolotov et al. studied equations equivalent to (5)-(6), although they considered identical oscillators so that $\sigma = 0$ and also took the limit $N \rightarrow \infty$. They were interested in chimera solutions which are spatially-inhomogeneous steady states of (8)-(9) and showed that such states satisfy several spatial ordinary differential equations (once the limit $N \rightarrow \infty$ has been taken). However, finding the stability of such states by linearising (8)-(9) about them was difficult due to the large number of eigenvalues near the imaginary axis resulting from their consideration of identical oscillators. Instead, stability was inferred from the results of long simulations of the equivalent of (1)-(2).

Smirnov et al. [30] also considered equations equivalent to (5)-(6), also with $\sigma = 0$ and in the limit $N \rightarrow \infty$. They showed that stable chimera solitons exist on an infinite domain, and these are described by homoclinic orbits in the spatial dynamics. They also considered a spatially-discrete model equivalent to (1)-(2) with $M = 1$ and all ω_j^k equal and found that the spatial discreteness caused the chimera solitons to move in an unusual “swaying” motion.

In earlier work [33], Smirnov et al. considered equations equivalent to (5)-(6) but with $\epsilon = 0$ which, as explained above, corresponds to nonlocal coupling of the a_j . They studied solitary synchronisation waves for which the local synchronisation level is higher than in the surrounding background.

2.1. Asymmetric coupling. The model (1)-(2) has symmetric local coupling, since the dynamics of z_j depend equally on both z_{j+1} and z_{j-1} . However, one could also

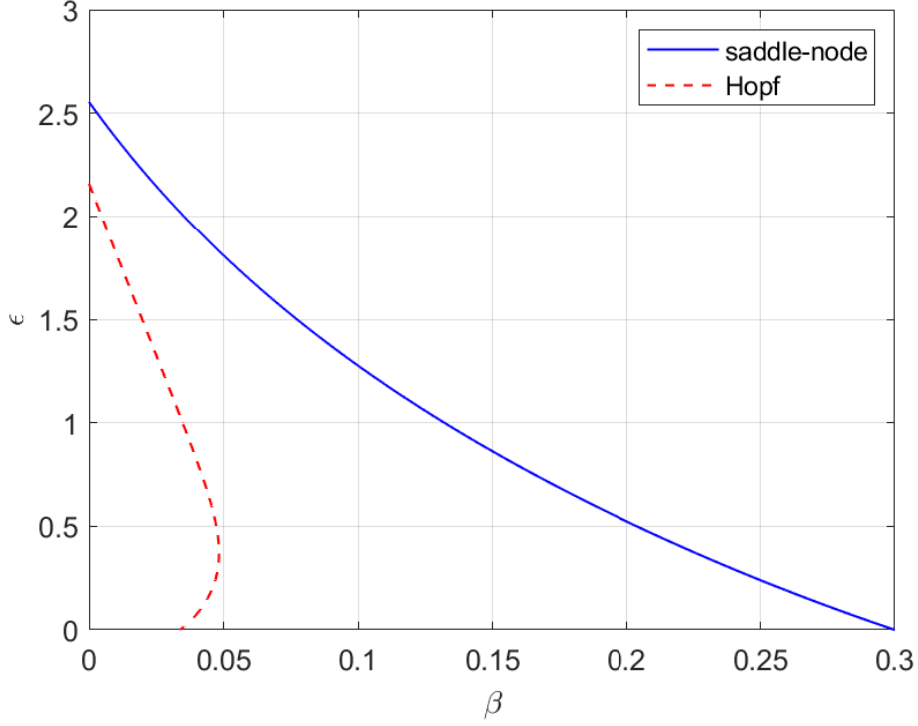


FIGURE 3. Bifurcations of chimera steady states of (8)-(9). The chimera is stable within the region bounded by the two curves. Parameters: $\omega_0 = 1$, $\sigma = 0.01$, $A = 1.5$, $L = 2\pi$, $N = 200$.

consider asymmetric local coupling. As an example we replace (2) by

$$(10) \quad \epsilon \frac{dz_j}{dt} = \frac{Ae^{i\beta}}{M} \sum_{k=1}^M e^{i\theta_j^k} - z_j + \frac{z_{j+1} - 2z_j + z_{j-1}}{(\Delta x)^2} + v \frac{z_j - z_{j-1}}{\Delta x}$$

where v is a constant. Clearly this new term is a finite-difference approximation to $\partial z / \partial x$. Setting $v \neq 0$ causes chimeras to move. Letting both M and N tend to infinity we obtain the equations

$$(11) \quad \frac{\partial a}{\partial t} = -(\sigma - i\omega_0)a - (i/2)(z + \bar{z}a^2)$$

$$(12) \quad \epsilon \frac{\partial z}{\partial t} = Ae^{i\beta}a - z + \frac{\partial^2 z}{\partial x^2} + v \frac{\partial z}{\partial x}$$

where a and z are now functions of x and t .

The solutions of interest are chimeras which move at a constant speed in x . We can *freeze* these moving solutions by going to a coordinate frame which is simultaneously translating at the speed of the chimeras and rotating at the same speed at each value of x [34, 35]. If c is the speed at which a chimera is moving and s is the speed of the rotating coordinate frame, then in this new coordinate frame (11)-(12) become

$$(13) \quad \frac{\partial a}{\partial t} = -(\sigma - i(\omega_0 - s))a - (i/2)(z + \bar{z}a^2) - c \frac{\partial a}{\partial x}$$

$$(14) \quad \epsilon \frac{\partial z}{\partial t} = Ae^{i\beta}a - z + \frac{\partial^2 z}{\partial x^2} + (v - \epsilon c) \frac{\partial z}{\partial x} - i\epsilon s z$$

We are interested in steady states of these equations. To solve them we need to add several “pinning” conditions to remove the invariance of solutions under both spatial translations and rotations of a and z in the complex plane [34]. We can find the stability of these steady states by linearising (13)-(14) about them.

Following a chimera steady state of (13)-(14) as v is varied we obtain the plot shown in Fig. 4(a). For small v the speed of the moving chimera initially increases as v does, but for larger values the plot of c versus v becomes multivalued. This phenomenon was first observed in [35]. (See also [36, 37, 38].) Moving chimeras are stable for small v but become unstable through a Hopf bifurcation at $v \approx 0.3$. This is in contrast to the moving chimeras in the nonlocally coupled system studied in [35], which lose and regain stability repeatedly as the branch of solutions is followed. Panels (b) and (c) of Fig. 4 show examples of profiles of $|a(x, t)|$ for a stable and unstable, respectively, moving chimera. As in [37, 35], the magnitude of a (i.e. the local level of synchrony of the phase oscillators) oscillates as one moves around the domain.

The travelling chimeras have an integer “twist” associated with them, since as the domain is traversed once, the argument of a must vary through an integer multiple of 2π . The twist of solutions on the curve shown in Fig. 4(a) starts at zero for small v and increases to 1 and 2 as v is increased (not shown).

In recent work [31], Smirnov and Pikovsky considered a model equivalent to (1) and (10) but with identical oscillators, $M = 1$, and $N \rightarrow \infty$. They set $\epsilon = 0$ which then creates *asymmetric* nonlocal coupling among the phase oscillators, similar to that in [37, 35]. They found travelling waves with varying twists and determined their stability, and also patterns described as travelling chimeras.

3. WINFREE OSCILLATORS IN 1D

As a second example we consider a network of Winfree oscillators [39, 40, 41]. The equations are

$$(15) \quad \frac{d\theta_j^k}{dt} = \omega_j^k + \kappa Q(\theta_j^k) u_j$$

$$(16) \quad \epsilon \frac{du_j}{dt} = \frac{1}{M} \sum_{k=1}^M P_n(\theta_j^k) - u_j + \frac{u_{j+1} - 2u_j + u_{j-1}}{(\Delta x)^2}$$

for $j = 1, 2, \dots, N$ and $k = 1, 2, \dots, M$, where θ_j^k is the phase of the k th oscillator in community j , and κ and ϵ are parameters. Note that each u_j is real. The functions Q and P_n are given by $Q(\theta) = \sin \beta - \sin(\theta + \beta)$ where β is a parameter, and $P_n(\theta) = a_n(1 + \cos \theta)^n$ where $a_n = 2^n(n!)^2/(2n)!$, and $\Delta x = L/N$ where L is the length of the domain. Periodic boundary conditions in space are used. $Q(\theta)$ is the phase response curve of the oscillator and can be measured experimentally for a neuron, for example [42]. As above, the ω_j^k are randomly chosen from the distribution (3).

An example of a chimera is shown in Fig. 5 where for simplicity we show the phase of only one oscillator at each lattice point. The incoherent group of oscillators is in the centre of the domain. A chimera in such a system was shown in [15], but no analysis of it was performed.

As above we can let $M \rightarrow \infty$ and use the Ott/Antonsen ansatz to derive equations describing the phase oscillator density in each community. Defining a_j as in (4) we find [43]

$$(17) \quad \frac{da_j}{dt} = \kappa u_j e^{-i\beta} / 2 + (i\omega_0 - \delta + i\kappa \sin(\beta) u_j) a_j - \kappa e^{i\beta} u_j a_j^2 / 2$$

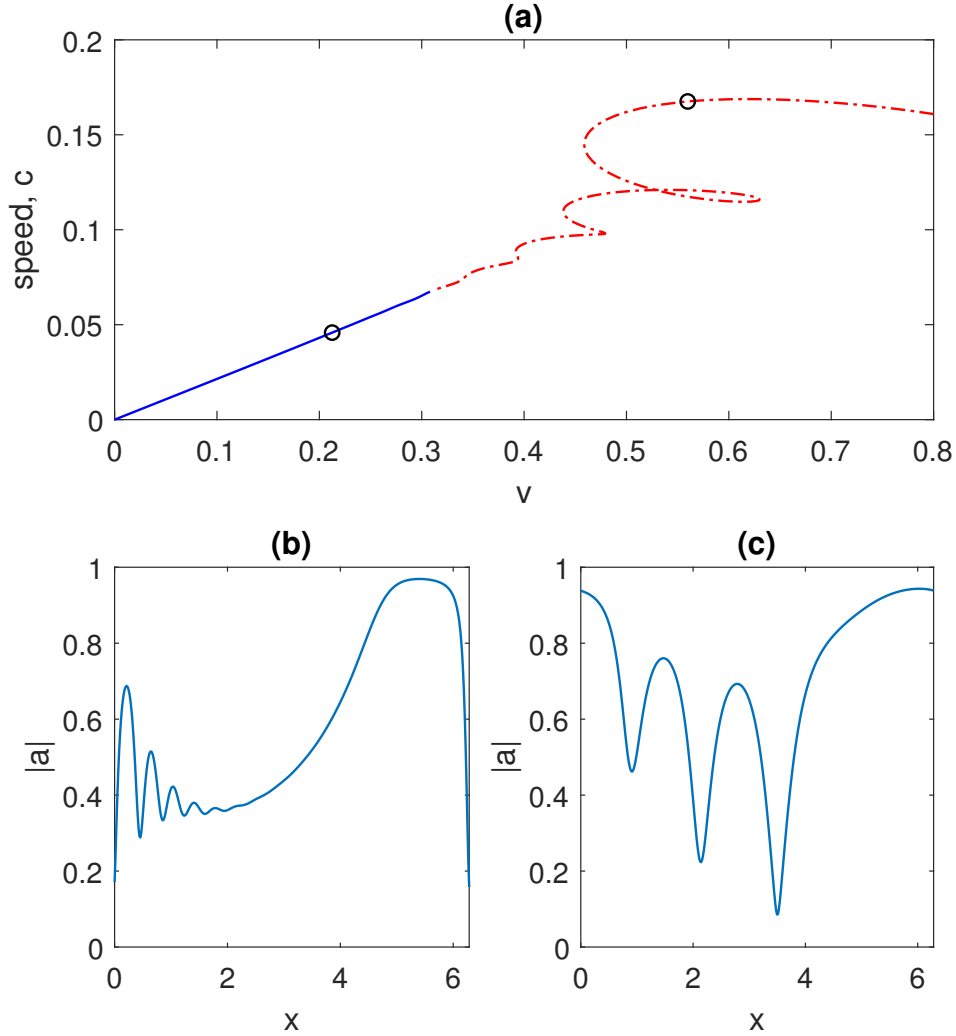


FIGURE 4. (a): Speed, c , of the travelling chimera solution of (11)-(12) as a function of the magnitude of the asymmetric coupling, v . Blue solid: stable; red dash-dotted: unstable. (b) and (c): snapshots of $|a(x,t)|$ at the points indicated by the black circles (left and right respectively) in panel (a). Both chimeras are moving to the left. Parameters: $\omega_0 = 1, \beta = 0.1, \epsilon = 0.2, \sigma = 0.01, A = 1.5, L = 2\pi$. The domain was discretised with 400 points.

Setting $n = 4$ we find that [44]

$$\lim_{M \rightarrow \infty} \frac{1}{M} \sum_{k=1}^M P_n(\theta_j^k) = 1 + \frac{4(a_j + \bar{a}_j)}{5} + \frac{2(a_j^2 + \bar{a}_j^2)}{5} + \frac{4(a_j^3 + \bar{a}_j^3)}{35} + \frac{a_j^4 + \bar{a}_j^4}{70} \equiv f(a_j, \bar{a}_j)$$

and thus the system is described by (17) and

$$(18) \quad \epsilon \frac{du_j}{dt} = f(a_j, \bar{a}_j) - u_j + \frac{u_{j+1} - 2u_j + u_{j-1}}{(\Delta x)^2}$$

Unlike the system studied in Sec. 2, equations (15)-(16) are not invariant under a uniform rotation of phases and thus the chimera shown in Fig. 5 corresponds to a periodic solution of (17) and (18) and must be studied as such.

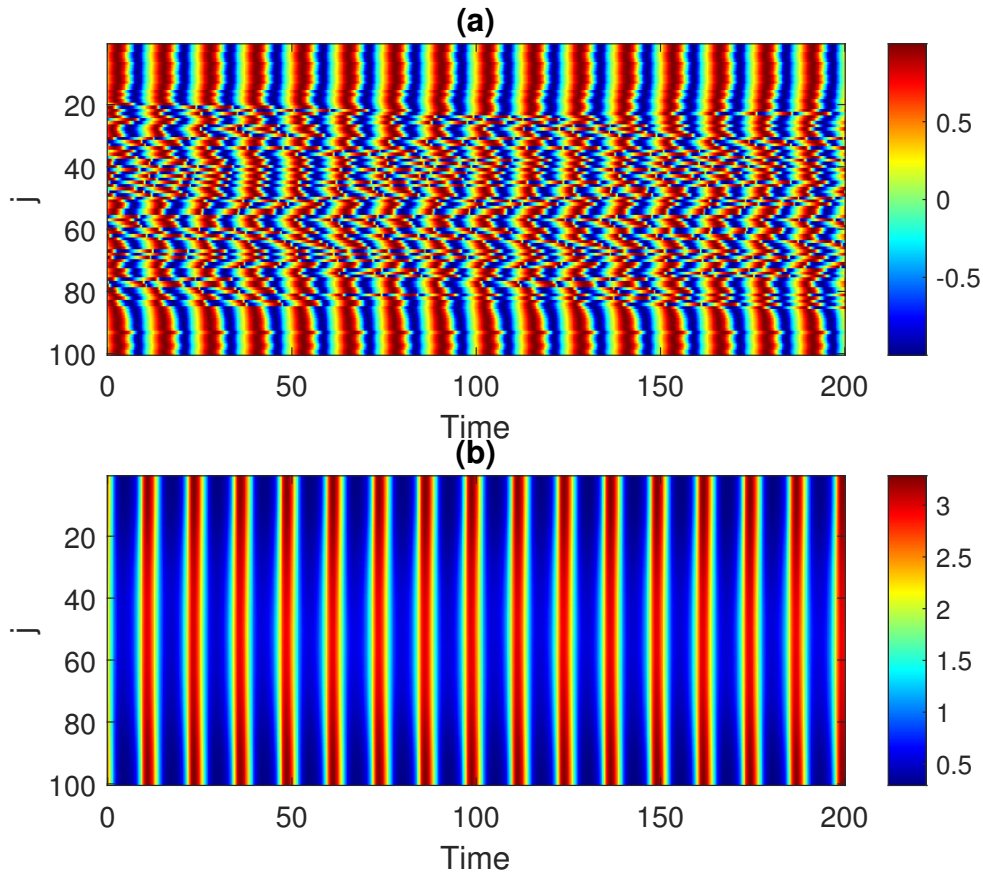


FIGURE 5. Chimera state in (15)-(16). (a): $\sin \theta_j^1$; (b): u_j . Parameters: $\omega_0 = 0.3, \beta = \pi/2 - 0.2, \kappa = 0.4, \epsilon = 0.1, \sigma = 0.001, n = 4, M = 20, N = 100, L = 4$.

One of the important parameters in a network of Winfree oscillators is the level of heterogeneity in natural frequencies, given here by δ . Varying δ and following both fixed points and periodic solutions of (17) and (18) we obtain Fig. 6. As in an all-to-all coupled network, for small κ and large δ the system has a stable spatially-uniform fixed point, indicated by the solid blue curve. As δ is decreased this state loses stability in a supercritical Hopf bifurcation, leading to a stable periodic solution, again with no spatial structure (shown with blue circles). As δ is decreased further this state loses stability to a solution which is periodic in time and which has some spatial structure: this is the chimera state corresponding to the type of solution shown in Fig. 5.

To represent the chimera we define a chimera index

$$(19) \quad \chi \equiv \frac{1}{T} \int_0^T \max_x(u(x, t)) - \min_x(u(x, t)) dt$$

where T is the period of the oscillation. For a spatially-uniform periodic state χ will be zero. In the inset of Fig. 6 we plot χ as a function of δ . We see that χ varies from 0 (at $\delta \approx 0.0075$) when the spatially-uniform period state loses stability to a maximum at $\delta = 0$, i.e. the chimera bifurcates in a supercritical way. The chimera is stable over the range of δ for which it exists.

Increasing κ with $\delta = 0.005$ and all other parameters the same as above, we see the same scenario (not shown).

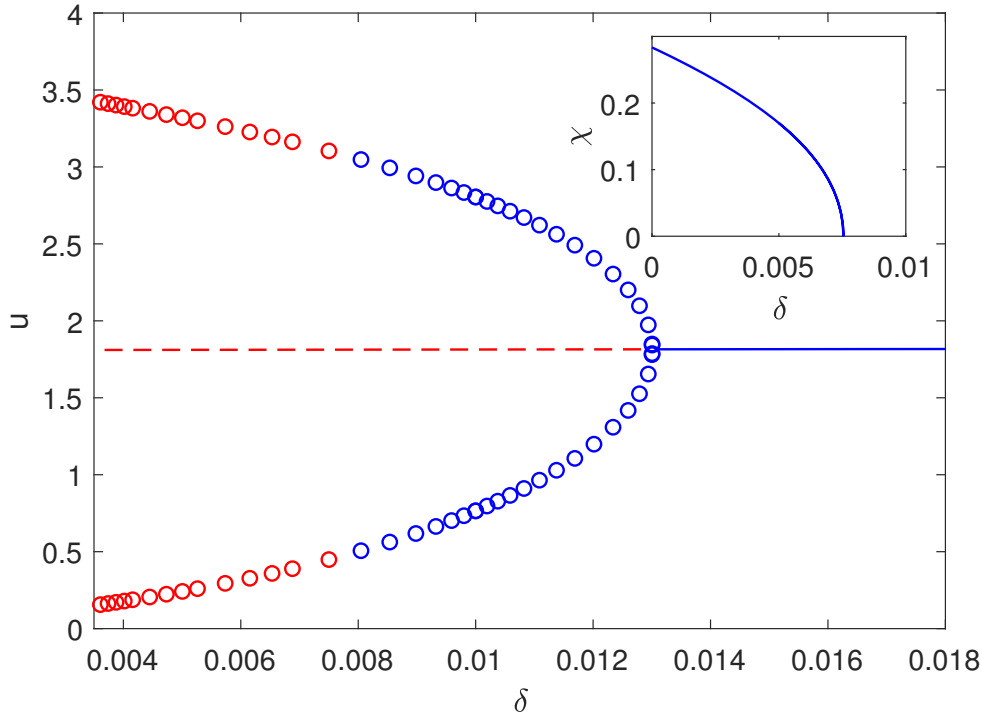


FIGURE 6. Fixed points and periodic solutions of (17) and (18). Lines show the value of u at a spatially-uniform fixed point (solid blue: stable; dashed red: unstable). Circles show the maximum and minimum of u over one period of a spatially-uniform periodic solution (blue: stable; red: unstable). The inset shows the chimera index χ defined in the text. Parameters: $\omega_0 = 0.3$, $\beta = \pi/2 - 0.2$, $\kappa = 0.4$, $\epsilon = 0.1$, $n = 4$, $M = 1$, $N = 100$, $L = 4$.

4. 2D SQUARE DOMAIN

The next system we consider is a two-dimensional square domain. Spiral wave chimeras have been observed in a number of two-dimensional networks with nonlocal coupling [45, 46, 47]. Our system is

$$(20) \quad \frac{d\theta_j^k}{dt} = \omega_j^k - \text{Im} \left[e^{i(\theta_j^k + \alpha)} z_j \right] = \omega_j^k + (i/2) \left[e^{i(\theta_j^k + \alpha)} z_j - e^{-i(\theta_j^k + \alpha)} \bar{z}_j \right]$$

$$(21) \quad \epsilon \frac{dz_j}{dt} = \frac{100}{M} \sum_{k=1}^M e^{-i\theta_j^k} + \nabla^2 z_j - z_j$$

where as above θ_j^k is the phase of the k th oscillator in community j and j is the index of a point in a 2D lattice. We use a five-point stencil to approximate the Laplacian on a regular $N \times N$ square grid and use zero-derivative Neumann boundary conditions. An example of a spiral wave chimera solution of (20)-(21) is shown in Fig. 7 where for simplicity we set $M = 1$. In the image of $\sin \theta_j^1$ the incoherent core is clearly visible. There is slight “speckling” in panel (a) due to the randomly chosen values of ω_j^1 . z is clearly a smooth function of space with a phase singularity where $|z| = 0$ at the centre of the spiral.

Taking the limit $M \rightarrow \infty$ and defining a_j to be the complex conjugate of the term on the right of (4) we have

$$\epsilon \frac{dz_j}{dt} = 100a_j + \nabla^2 z_j - z_j$$

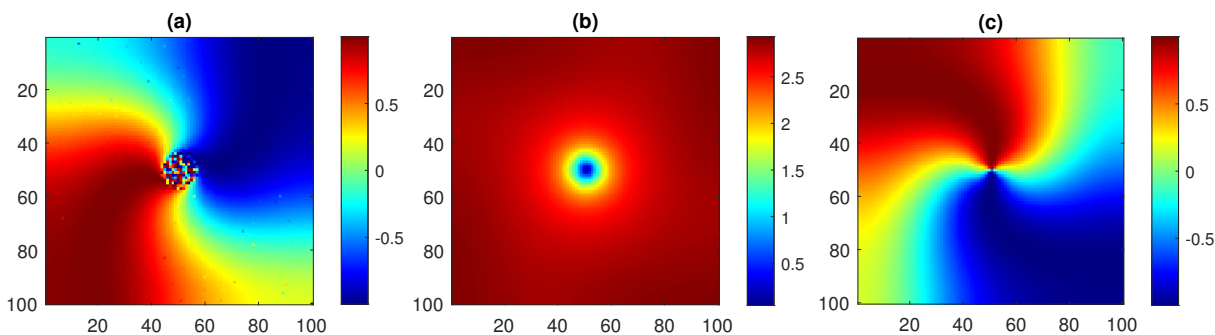


FIGURE 7. Snapshot of a spiral wave chimera solution of (20)-(21). (a): $\sin \theta_j^1$; (b): $|z_j|$; (c): $\sin(\arg(z_j))$. Parameters: $\omega_0 = 0, \alpha = 0.7\pi, \sigma = 0.001, \epsilon = 20, M = 1, N = 100, L = 3$.

and

$$\frac{da_j}{dt} = z_j e^{i\alpha}/2 - (\sigma + i\omega_0)a_j - \bar{z}_j e^{-i\alpha} a_j^2/2$$

The solutions of interest are stationary in a rotating coordinate frame, i.e. we are interested in fixed points of

$$(22) \quad \frac{da_j}{dt} = z_j e^{i\alpha}/2 - (\sigma + i\omega_0)a_j - \bar{z}_j e^{-i\alpha} a_j^2/2 - i\Omega a_j$$

$$(23) \quad \epsilon \frac{dz_j}{dt} = 100a_j + \nabla^2 z_j - z_j - \epsilon i\Omega z_j$$

where Ω is the speed of the rotating coordinate frame.

Following such a fixed point as α is varied we obtain the results in Fig. 8. One interesting result is that unlike other systems, the spiral persists for α greater than $\pi/2$. Another interesting result is shown in panel (b) where the radius of the incoherent core is plotted. In other systems this increased linearly with α , at least for small α . Here, the core does not really develop until $\alpha \approx 1.3$. (The incoherent core was defined as grid points for which $|a_j| < 0.95$. Since N is odd there is always at least one lattice point, in the centre of the spiral, for which $|a_j| < 0.95$, and thus this radius is never zero.)

5. ANNULUS

One type of domain on which chimeras have recently been studied is the annulus [48]. Laing previously investigated both multi-headed chimeras and rotating waves in networks of nonlocally coupled phase oscillators on an annulus [48]. (Also see [49].)

The model we consider is

$$(24) \quad \frac{d\theta_j^k}{dt} = \omega_j^k - \text{Im} \left[e^{i(\theta_j^k + \alpha)} z_j \right] = \omega_j^k + (i/2) \left[e^{i(\theta_j^k + \alpha)} z_j - e^{-i(\theta_j^k + \alpha)} \bar{z}_j \right]$$

$$(25) \quad \epsilon \frac{dz_j}{dt} = \frac{50}{M} \sum_{k=1}^M e^{-i\theta_j^k} + \nabla^2 z_j - z_j$$

where as above θ_j^k is the phase of the k th oscillator in community j and j is the index of a point on the annulus with inner radius a and outer radius b . The domain is discretised with N_r points in the radial direction and N_ϕ in the angular direction. Second derivatives in the angular and radial directions were implemented as in (2) and the first derivative in the radial direction was implemented using a centred finite difference. Importantly, Dirichlet boundary conditions are used for z , where $z = 0$ on both the inner and outer boundaries.

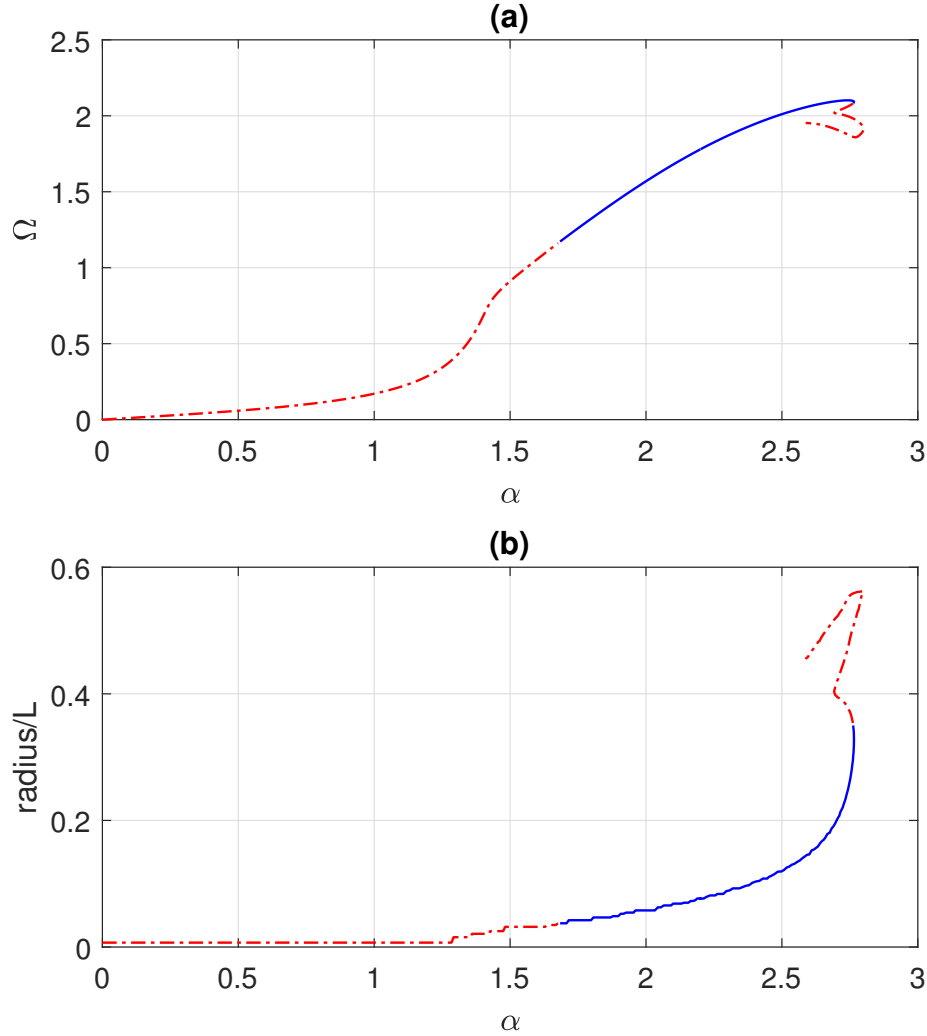


FIGURE 8. Continuation in α of a spiral wave chimera steady state of (22)-(23). (a): Ω versus α . (b): radius of incoherent core, divided by domain side length L , versus α . Blue solid: stable; red dash-dotted: unstable. Parameters: $\omega_0 = 0, \sigma = 0.03, \epsilon = 20, N = 81, L = 3$.

An example of a rotating wave solution of (24)-(25) is shown in Fig. 9. In the plot of $\sin \theta_j^1$ we see incoherent regions near the inner and outer boundaries of the domain, while θ_j^1 increases through 4π as we move in the angular direction around the domain, away from the boundaries. The phase θ_j^1 will vary through a multiple of 2π as we move around the domain, and in this case that multiple is $n = 2$, referred to as the winding number. We see that z is continuous in space.

The reason for the oscillators near the boundaries being incoherent is easy to see: oscillators at point j feel the field z_j and if $|z_j|$ is small, the oscillators will not lock to it. Since z is continuous in space and equal to zero at the boundaries, there must be some incoherent oscillators near the boundaries.

As in Sec. 4, in the limit $M \rightarrow \infty$, the solutions of interest are fixed points of

$$(26) \quad \frac{da_j}{dt} = z_j e^{i\alpha} / 2 - (\sigma + i\omega_0) a_j - \bar{z}_j e^{-i\alpha} a_j^2 / 2 - i\Omega a_j$$

$$(27) \quad \epsilon \frac{dz_j}{dt} = 50a_j + \nabla^2 z_j - z_j - i\epsilon\Omega z_j$$

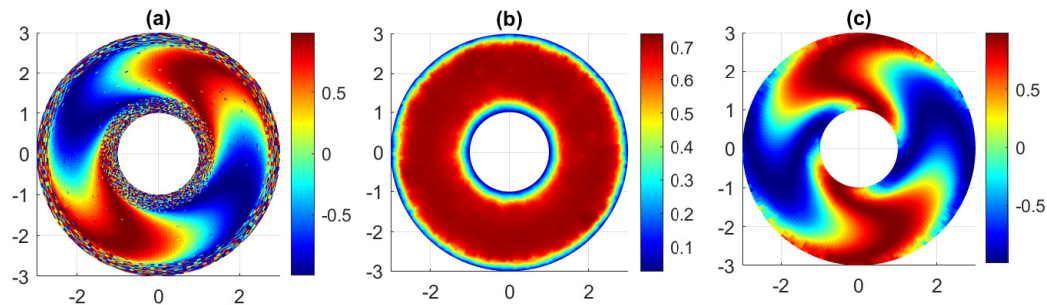


FIGURE 9. Snapshot of a rotating wave solution of (24)-(25) with $n = 2$. (a): $\sin \theta_j^1$; (b): $|z_j|$; (c): $\sin(\arg(z_j))$. Parameters: $\omega_0 = 0, \alpha = 2.7, \sigma = 0.001, \epsilon = 100, M = 1, a = 1, b = 3$. $N_r = 100, N_\phi = 180$.

where Ω is the speed of the rotating coordinate frame.

We followed rotating waves with $n = 0, 1, 2, 3$ as α was varied, and the results are shown in Fig. 10. Only the $n = 0, 1$ curves persist down to $\alpha = 0$, others have saddle-node bifurcations. The $n = 0$ curve is always stable, and the other curves are only stable for $\sim 1.5 < \alpha < \sim 2.5$. These results are fundamentally different in several ways from those for nonlocally coupled oscillators found in [48]: here

- the curves do not all persist down to $\alpha = 0$,
- the curves persist past $\alpha = \pi/2$,
- curves for different n are not simply related by scaling Ω (and here the value of Ω increases with n whereas in [48] it decreases).

6. SUMMARY

We studied a number of networks of phase oscillators where at each node there are many phase oscillators and one auxiliary variable, which may be real or complex. The only coupling between nodes is nearest-neighbour coupling of the auxiliary variables. These networks are capable of supporting stable chimera states, for which oscillators in part of the domain are largely synchronous, while those in the rest are more asynchronous. All of these systems can be studied using the Ott/Antonsen ansatz applied to the phase oscillator populations, and we obtain a set of coupled equations for both the Kuramoto order parameter and the value of the auxiliary variable at each node. Steady states of these equations correspond to chimeras, and their stability and bifurcations can thus be determined straight-forwardly.

We first examined several one-dimensional networks previously studied in [48], but now we can properly determine the stability of chimeras found in those networks. For the Kuramoto oscillators (Sec. 2) adding local asymmetric coupling caused the chimera to move around the domain. Interestingly, the chimera's speed is not a monotonic function of the asymmetric coupling strength, a phenomenon seen previously only in systems with nonlocal coupling [35, 36, 37, 38]. For the Winfree oscillators (Sec. 3) we showed how the chimera arises as the result of several bifurcations as the heterogeneity of the uncoupled oscillators' frequencies decreased. We then considered a spiral wave chimera in a square domain (Sec. 4). In contrast with many other spiral wave chimeras found in nonlocally coupled systems [50, 46, 47, 51, 52], the spiral wave chimera found

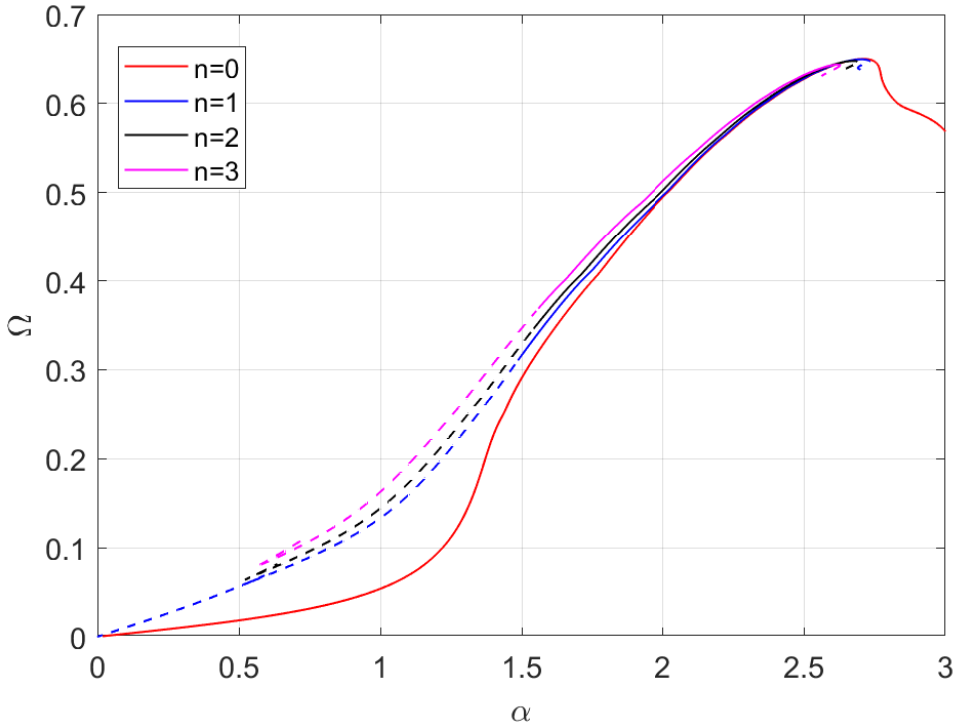


FIGURE 10. Rotation speed Ω as a function of α for rotating waves with winding numbers $n = 0, 1, 2, 3$. Solid curves: stable; dashed: unstable. Parameters: $\omega_0 = 0, \sigma = 0.001, \epsilon = 100, M = 1, a = 1, b = 3$. $N_r = 60, N_\phi = 100$.

here (i) exists for α significantly past $\alpha = \pi/2$ and (ii) does not have a core whose size grows linearly with α (for small α). The last system considered was an annular domain, for which we studied rotating waves. While these patterns do have some coherent and some incoherent oscillators, they should not be considered chimeras, as the incoherent oscillators are near the boundaries of the domain, where the auxiliary variable must have a small magnitude due to the boundary conditions.

For both two-dimensional domains (Secs. 4 and 5) we found that solutions of interest are fundamentally different in several ways from those for which coupling is nonlocal. These results add to our knowledge of the types of dynamics seen in networks, and invite further investigations into the similarities and differences in the dynamics of networks with local and nonlocal coupling [53].

REFERENCES

- [1] Oleh E Omel'chenko. The mathematics behind chimera states. *Nonlinearity*, 31(5):R121, 2018.
- [2] Mark J Panaggio and Daniel M Abrams. Chimera states: Coexistence of coherence and incoherence in networks of coupled oscillators. *Nonlinearity*, 28(3):R67, 2015.
- [3] Erik Andreas Martens, Shashi Thutupalli, Antoine Fourrière, and Oskar Hallatschek. Chimera states in mechanical oscillator networks. *Proceedings of the National Academy of Sciences*, 110(26):10563–10567, 2013.
- [4] Jan Frederik Tetz, Julian Rode, Mark R Tinsley, Kenneth Showalter, and Harald Engel. Spiral wave chimera states in large populations of coupled chemical oscillators. *Nature Physics*, 14(3):282–285, 2018.
- [5] Edward Ott and Thomas M. Antonsen. Low dimensional behavior of large systems of globally coupled oscillators. *Chaos*, 18(3):037113, 2008.

- [6] Edward Ott and Thomas M. Antonsen. Long time evolution of phase oscillator systems. *Chaos*, 19(2):023117, 2009.
- [7] S.H. Strogatz. From Kuramoto to Crawford: exploring the onset of synchronization in populations of coupled oscillators. *Physica D*, 143(1-4):1–20, 2000.
- [8] Y. Kuramoto. *Chemical Oscillations, Waves, and Turbulence*. Springer, Berlin, 1984.
- [9] D.M. Abrams, R. Mirollo, S.H. Strogatz, and D.A. Wiley. Solvable model for chimera states of coupled oscillators. *Phys. Rev. Lett.*, 101(8):084103, 2008.
- [10] Carlo R. Laing. Chimera states in heterogeneous networks. *Chaos*, 19(1):013113, 2009.
- [11] Y. Kuramoto and D. Battogtokh. Coexistence of Coherence and Incoherence in Nonlocally Coupled Phase Oscillators. *Nonlinear Phenom. Complex Syst*, 5(4):380–385, 2002.
- [12] D.M. Abrams and S.H. Strogatz. Chimera states in a ring of nonlocally coupled oscillators. *Int. J. Bifurcat. Chaos*, 16(1):21–37, 2006.
- [13] Y. Kuramoto and S. Shima. Rotating spirals without phase singularity in reaction-diffusion systems. *Progr. Theor. Phys. Suppl.*, 150:115, 2003.
- [14] Sindre W Haugland. The changing notion of chimera states, a critical review. *Journal of Physics: Complexity*, 2(3):032001, 2021.
- [15] Carlo R Laing. Chimeras in networks with purely local coupling. *Physical Review E*, 92(5):050904, 2015.
- [16] Zachary G. Nicolaou, Hermann Riecke, and Adilson E. Motter. Chimera states in continuous media: Existence and distinctness. *Phys. Rev. Lett.*, 119:244101, Dec 2017.
- [17] MG Clerc, Saliya Coulibaly, MA Ferré, MA García-Ñustes, and RG Rojas. Chimera-type states induced by local coupling. *Physical Review E*, 93(5):052204, 2016.
- [18] Vladimir García-Morales, José A Manzanares, and Katharina Krischer. Chimera states under genuine local coupling. *Chaos, Solitons & Fractals*, 165:112808, 2022.
- [19] Tasso J Kaper and Theodore Vo. A new class of chimeras in locally coupled oscillators with small-amplitude, high-frequency asynchrony and large-amplitude, low-frequency synchrony. *Chaos: An Interdisciplinary Journal of Nonlinear Science*, 31(12):123111, 2021.
- [20] Bidesh K. Bera and Dibakar Ghosh. Chimera states in purely local delay-coupled oscillators. *Phys. Rev. E*, 93:052223, May 2016.
- [21] Johanne Hizanidis, Nikos Lazarides, and Giorgos P Tsironis. Chimera states in networks of locally and non-locally coupled squids. *Frontiers in Applied Mathematics and Statistics*, 5:33, 2019.
- [22] MG Clerc, Saliya Coulibaly, MA Ferré, and RG Rojas. Chimera states in a duffing oscillators chain coupled to nearest neighbors. *Chaos: An Interdisciplinary Journal of Nonlinear Science*, 28(8):083126, 2018.
- [23] Dmitrii Sergeevich Shchapin, AS Dmitrichev, and Vladimir Isaakovich Nekorkin. Chimera states in an ensemble of linearly locally coupled bistable oscillators. *JETP Letters*, 106:617–621, 2017.
- [24] Bing-Wei Li and Hans Dierckx. Spiral wave chimeras in locally coupled oscillator systems. *Physical Review E*, 93(2):020202, 2016.
- [25] Xiaodong Tang, Tao Yang, Irving R Epstein, Yang Liu, Yuemin Zhao, and Qingyu Gao. Novel type of chimera spiral waves arising from decoupling of a diffusible component. *The Journal of chemical physics*, 141(2):024110, 2014.
- [26] Lei Yang, Yuan He, and Bing-Wei Li. Spiral wave chimeras in populations of oscillators coupled to a slowly varying diffusive environment. *Frontiers of Physics*, 18(1):13309, 2023.
- [27] Anna Zakharova. *Chimera Patterns in Networks*. Springer, 2020.
- [28] Seon Choe, In-Ho Pak, Hyok Jang, Ryong-Son Kim, and Chol-Ung Choe. Self-emerging symmetry breakings in a two-population network of phase oscillators interacting via an external environment. *Physica D: Nonlinear Phenomena*, 440:133483, 2022.
- [29] DI Bolotov, MI Bolotov, LA Smirnov, GV Osipov, and AS Pikovsky. Synchronization regimes in an ensemble of phase oscillators coupled through a diffusion field. *Radiophysics and Quantum Electronics*, 64(10):709–725, 2022.
- [30] LA Smirnov, MI Bolotov, DI Bolotov, GV Osipov, and A Pikovsky. Finite-density-induced motility and turbulence of chimera solitons. *New Journal of Physics*, 24(4):043042, 2022.
- [31] L Smirnov and A Pikovsky. Travelling chimeras in oscillator lattices with advective–diffusive coupling. *Philosophical Transactions of the Royal Society A*, 381(2245):20220076, 2023.
- [32] Carlo R Laing. Chimeras on a ring of oscillator populations. *Chaos: An Interdisciplinary Journal of Nonlinear Science*, 33(1):013121, 2023.

- [33] L. A. Smirnov, G. V. Osipov, and A. Pikovsky. Solitary synchronization waves in distributed oscillator populations. *Phys. Rev. E*, 98:062222, Dec 2018.
- [34] Carlo R. Laing. Fronts and bumps in spatially extended kuramoto networks. *Physica D*, 240(24):1960 – 1971, 2011.
- [35] OE Omel’chenko. Travelling chimera states in systems of phase oscillators with asymmetric nonlocal coupling. *Nonlinearity*, 33(2):611, 2020.
- [36] Carlo R Laing and Oleh Omel’chenko. Moving bumps in theta neuron networks. *Chaos: An Interdisciplinary Journal of Nonlinear Science*, 30(4):043117, 2020.
- [37] OE Omel’chenko. Traveling chimera states. *Journal of Physics A: Mathematical and Theoretical*, 52(10):104001, 2019.
- [38] OE Omel’chenko. Periodic orbits in the ott–antonsen manifold. *Nonlinearity*, 36(2):845, 2022.
- [39] Diego Pazó and Ernest Montbrió. Low-dimensional dynamics of populations of pulse-coupled oscillators. *Physical Review X*, 4:011009, Jan 2014.
- [40] Joel T Ariaratnam and Steven H Strogatz. Phase diagram for the winfree model of coupled nonlinear oscillators. *Physical Review Letters*, 86(19):4278, 2001.
- [41] Arthur T Winfree. Biological rhythms and the behavior of populations of coupled oscillators. *Journal of theoretical biology*, 16(1):15–42, 1967.
- [42] Nathan W Schultheiss, Astrid A Prinz, and Robert J Butera. *Phase response curves in neuroscience: theory, experiment, and analysis*. Springer, 2011.
- [43] Carlo R Laing. Phase oscillator network models of brain dynamics. *Computational models of brain and behavior*, pages 505–517, 2017.
- [44] Shawn Means and Carlo R Laing. Explosive behaviour in networks of winfree oscillators. *Chaos, Solitons & Fractals*, 160:112254, 2022.
- [45] Oleh E Omel’chenko, Matthias Wolfrum, Serhiy Yanchuk, Yuri L Maistrenko, and Oleksandr Suddakov. Stationary patterns of coherence and incoherence in two-dimensional arrays of non-locally-coupled phase oscillators. *Physical Review E*, 85(3):036210, 2012.
- [46] Erik A. Martens, Carlo R. Laing, and Steven H. Strogatz. Solvable model of spiral wave chimeras. *Phys. Rev. Lett.*, 104(4):044101, Jan 2010.
- [47] Jianbo Xie, Edgar Knobloch, and Hsien-Ching Kao. Twisted chimera states and multicore spiral chimera states on a two-dimensional torus. *Phys. Rev. E*, 92:042921, Oct 2015.
- [48] Carlo R Laing. Chimeras on annuli. *Chaos: An Interdisciplinary Journal of Nonlinear Science*, 32(8):083105, 2022.
- [49] Yujie Ding and Bard Ermentrout. Rotating waves of nonlocally coupled oscillators on the annulus. *SIAM Journal on Applied Dynamical Systems*, 21(3):2047–2079, 2022.
- [50] Carlo R. Laing. The dynamics of chimera states in heterogeneous Kuramoto networks. *Physica D*, 238(16):1569–1588, 2009.
- [51] Mark J Panaggio and Daniel M Abrams. Chimera states on the surface of a sphere. *Physical Review E*, 91(2):022909, 2015.
- [52] Carlo R Laing. Chimeras in two-dimensional domains: heterogeneity and the continuum limit. *SIAM Journal on Applied Dynamical Systems*, 16(2):974–1014, 2017.
- [53] C. R. Laing. Spiral waves in nonlocal equations. *SIAM Journal on Applied Dynamical Systems*, 4(3):588–606, 2005.

Email address: `c.r.laing@massey.ac.nz`

SCHOOL OF MATHEMATICAL AND COMPUTATIONAL SCIENCES, MASSEY UNIVERSITY, PRIVATE BAG 102-904 NSMC, AUCKLAND, NEW ZEALAND., PHONE: +64-9-414 0800 EXTN. 43512 FAX: +64-9-443 9790